LINEAR AND NON-LINEAR OPTICS OPTIMISATION FOR THE DIAMOND-II STORAGE RING

N. Blaskovic Kraljevic*, H. Ghasem, I.P.S. Martin, B. Singh,
Diamond Light Source, Oxfordshire, UK

Abstract

The design performance of the 3.5 GeV Diamond-II low-emittance electron storage ring has been studied as a function of the linear and non-linear lattice tuning parameters. A Multi-Objective Genetic Algorithm (MOGA) has been implemented and refined to optimise both the beam lifetime and the injection efficiency for off-axis injection. The sextupole magnets have been further split into ten families, according to their local linear optics, with each family varied independently as part of the MOGA optimisation; if necessary, the resulting chromaticity is corrected with a subset of the sextupoles to be within an operational range. In addition, the tune and the strengths of the two families of octupoles have been varied as part of the MOGA search. The simulations have been run on 5 machine error seeds, including misalignment, field strength and multipole errors, to obtain a solution which is robust against machine imperfections. The results of the optimisation are presented alongside a comparison of the baseline performance.

INTRODUCTION

The beam lifetime and injection efficiency (IE) of the Diamond-II storage ring [1] has been further optimised by varying the sextupole and octupole strengths. The work presented here builds on the Multi-Objective Genetic Algorithm (MOGA) implemented previously [2], but on this occasion the sextupole families have been subdivided according to their local linear optics. No hardware change is required as each sextupole will be on an individual power supply.

The Diamond-II storage ring design consists of six identical super-periods, with adjacent super-periods separated by a long (L) straight. Each super-period consists of four cells, with adjacent cells within a super-period separated by a standard (S) straight. Each cell also contains a mid (M) straight at its centre [1].

As the linear optics is different according to if the end of the cell is adjacent to a long or standard straight (Fig. 1), the four families of sextupoles S1 to S4 have been subdivided with those closest to a long straight renamed as SnL (with $n = 1, 2, 3, 4$). The remaining sextupoles preserve the existing naming convention where SnA (with $n = 2, 3, 4$) are chromatic sextupoles at high dispersion locations, used primarily to correct chromaticity, and SnX (with $n = 1, 5, 6$) are harmonic sextupoles, used to maximise the dynamic aperture (Fig. 1).

SIMULATION

The Diamond-II storage ring lattice in Accelerator Toolbox (AT2) [3] was used, including apertures for closed collimators and insertion devices (IDs). A radiofrequency (RF) voltage of 1.42 MV was used in the first instance, without a harmonic cavity. Random errors were applied to each of five machine seeds consisting of Δx, Δy transverse misalignment errors, roll errors and fractional strength errors; the 'reduced' errors used [4] replicate the final, corrected machine performance after all optics corrections steps have been applied, without needing to conduct the lengthy and time-consuming commissioning procedure [1]. In addition, random and systematic multipole errors were added to quadrupoles and sextupoles.

The simulation procedure [2] includes orbit, tune and chromaticity correction. For each possible lattice solution, the tune was corrected to the nominal value of $(\nu_x, \nu_y) = (54.14, 20.24)$ using five families of quadrupoles located in dispersion-free regions at the ends of the standard and long straights (Q1N, Q2N, Q0L, Q1L and Q2L). The chromaticity was corrected using all families of chromatic sextupoles only if the chromaticity was either below 2 (in which case it was corrected to 2) or above 5 (in which case it was corrected to 5), to ensure that the chromaticity is large enough to mitigate transverse instabilities [5] and that it is small enough for an optimum efficacy of the transverse multi-bunch feedback.

* neven.blaskovic-kraljevic@diamond.ac.uk

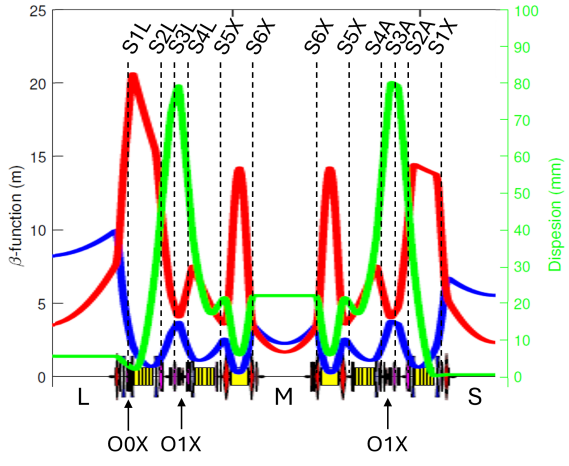

Figure 1: Horizontal (blue) and vertical (red) β functions and dispersion in the first cell between a long (L) and standard (S) straight [1], indicating the location of the sextupoles and octupoles.

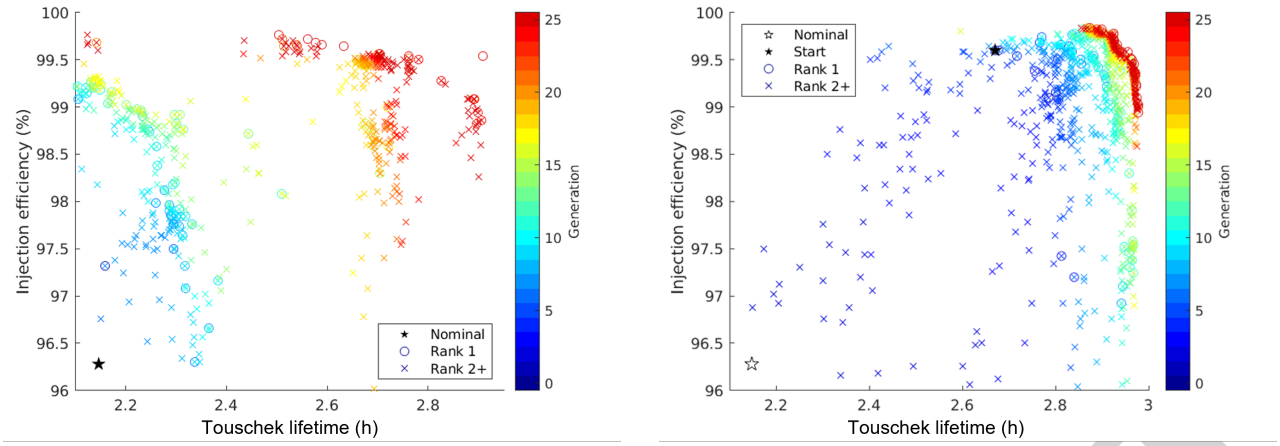

(a) (b)

Figure 2: Pareto front (∘) and higher-ranked solutions (×) in the IE vs. lifetime objective function space for (a) Run 1 and (b) Run 2 (generation numbers are colour-coded). Each solution is the average of five machine error seeds.

The Touschek lifetime was calculated in the first instance using Bruck's formula [6] by computing the momentum aperture at the sextupoles after tracking a stored beam for 512 turns. Measuring at the sextupoles provides a representative sampling of the lattice, including high-dispersion locations where the momentum acceptance is smallest, without having to measure at all elements.

The IE was evaluated by injecting a beam at a -4.5 mm offset and computing the fraction of particles successfully stored after 512 turns. Note that, whilst the Diamond-II design calls for a -4 mm off-axis injection, a larger offset was intentionally used in simulation to account for injected beam steering errors and enhance the losses. The relatively small number of turns used in the tracking was chosen to speed up computation time and is sufficient to see trends in the results.

MOGA SEARCH

A series of two successive MOGA optimisation runs were performed, each with 25 generations and 100 candidate solutions per generation. The first run used the nominal magnet strengths as a starting point, with a search space around each magnet's nominal value as given in Table 1. The Pareto front in Fig. 2a shows a 35% improvement in lifetime and an increase in IE to above 99.5% after 25 generations. As shown in Table 2, the best solution also has a higher chromaticity, in line with our previous chromaticity scans [2, 7].

In order to explore the sextupole and octupole space further, without necessarily relying on a higher chromaticity, the best solution of Run 1 was taken and its chromaticity was corrected down to the nominal value $(\xi_x, \xi_y) = (2.59, 2.62)$, and was used as the starting solution for MOGA Run 2 (Fig. 2b). The numbers quoted in Table 2 are those obtained for five random machine error seeds, with the mean chromaticity of the five seeds being given. Reducing the chromaticity to nominal does reduce the lifetime, but this is still significantly higher than that of the nominal lattice.

For Run 2, the sextupole and octupole search space was reduced and recentred on the Run 2 starting solution (as given in Table 1), as the best solutions were expected close to the previously identified optimum settings. The best solutions from Run 2 have a slightly longer lifetime than the best solution from Run 1 (Table 2). It is likely that a similar lifetime would have been achieved by extending the number of generations used for Run 1. In the case of Run 2, the chromaticity of the best solutions are all at the allowed limits of $(\xi_x, \xi_y) = (2, 5)$. The solution with the highest lifetime with an IE over 99.3% was selected as the best solution. In order to benchmark the results of this new solution whilst excluding the effect of the change in chromaticity, the chromaticity was corrected back down to the nominal value, producing the new baseline solution going forwards. The new baseline

Table 1: Maximum Operating Ranges and Allowed Search Ranges Around Start Values for Sextupole and Octupole Families, in AT2 Units

Magnets	Units	Full range	Search range Run 1	Search range Run 2
S1, S2, S5X, S6X	m^{-3}	±300	±100	±25
S3, S4	m^{-3}	±425	±100	±25
O0X	m^{-4}	±2955	±300	±150
O1X	m^{-4}	±6000	±300	±150

Table 2: Lifetime, IE, Horizontal (ξ_x) and Vertical Chromaticity (ξ_y) for Various MOGA Solutions

	Lifetime (h)	IE (%)	ξ_x	ξ_y
Nominal	2.16 ± 0.02	97.32 ± 0.29	2.59	2.62
Best Run 1	2.91 ± 0.02	99.54 ± 0.09	3.51	5.00
Start Run 2	2.67 ± 0.04	99.60 ± 0.06	2.52	2.77
Best Run 2	> 2.96	> 99.30	2.00	5.00
New baseline	2.62 ± 0.05	99.82 ± 0.04	2.52	2.72

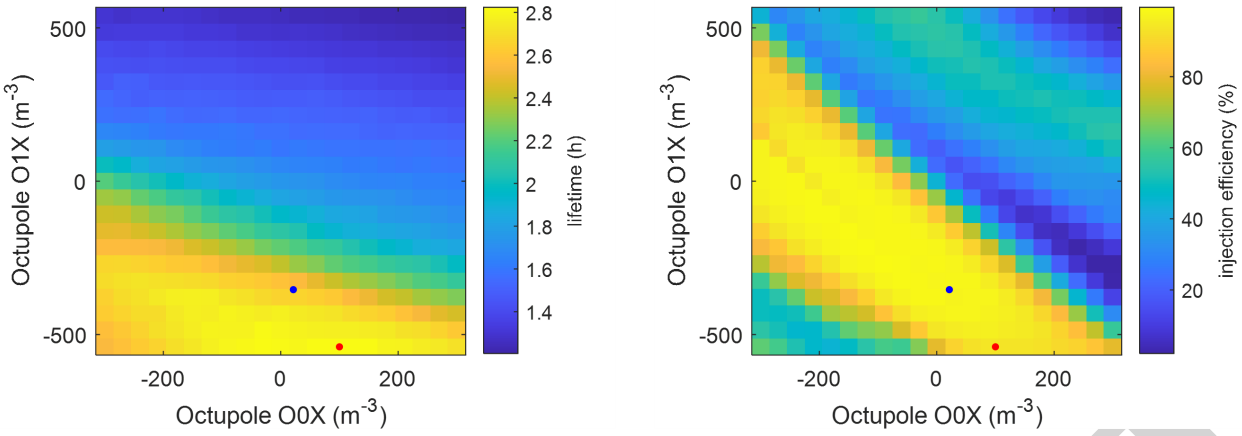

(a) (b)

Figure 3: (a) Lifetime and (b) IE for the octupole scan, averaging over five machine error seeds. The axes show the integrated octupole strengths (integrated over an O0X length of 0.10 m and an O1X length of 0.09 m). The blue dot shows the baseline solution obtained by MOGA; the red dot shows the optimised solution obtained from this scan.

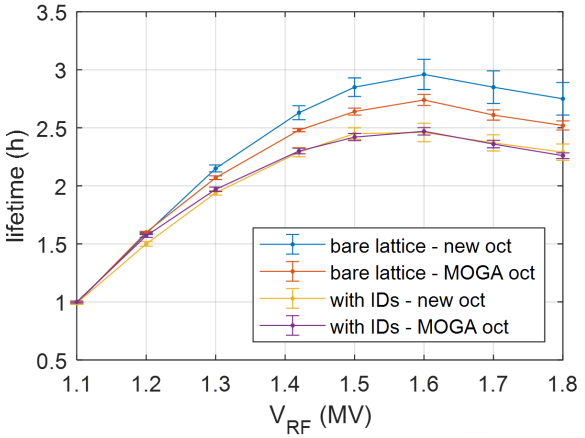

Figure 4: Lifetime as a function of RF voltage V_{RF}.

values in Table 2 were recalculated independently in AT2 with a fresh set of five seeds to confirm the results using Piwinski's lifetime formula [8], and increasing the number of turns in the simulation to 2500 turns for the lifetime and 1000 turns for the IE.

FURTHER OPTIMISTION

The new baseline solution was further refined by scanning the octupole strengths and adjusting the RF voltage. All results in this section make use of 2500 turns to obtain the lifetime and 1000 turns for the IE to produce reliable results.

Octupole Scan

Analysis of the search space of MOGA Run 2 identified that some alternative good solutions were located at the edges of the restricted octupole search range. To investigate this further, the new baseline lattice was taken and the lifetime and IE were computed for a detailed grid scan across the full range of both octupole families. As shown in Fig. 3, an optimised solution with improved lifetime was identified by increasing the O0X strength to 1000 m^{-4} and setting the O1X strength at the limit of -6000 m^{-4}. These results were generated using an RF voltage of 1.5 MV.

RF Voltage Scan

The effect of adding the kick maps for IDs and wigglers was included. The simulation procedure includes performing three iterations of Linear Optics from Closed Orbits (LOCO) correction with the two superconducting wigglers energised, then closing the remaining IDs and correcting the tunes back to nominal [9]. The results using both the new baseline octupole strengths from MOGA, and the optimised octupole strengths from the detailed 2D scan, are presented in Fig. 4, showing that a best lifetime of 2.96 ± 0.13 h (without ID kick maps) or 2.46 ± 0.08 h (with ID kick maps) can be achieved by increasing the RF voltage from 1.42 MV to 1.6 MV.

CONCLUSIONS

The Diamond-II lattice has been optimised to further improve the lifetime and IE. Subdividing the sextupole families according to their linear optics, and using a MOGA optimisation, has significantly improved both lifetime and IE. A detailed scan of the two octupole families and increasing the RF voltage from 1.42 MV to 1.6 MV to benefit from the increased momentum acceptance yields a best lifetime of 2.96 ± 0.13 h (without ID kick maps) or 2.46 ± 0.08 (with ID kick maps), without a harmonic cavity. A further increase in lifetime would be possible by allowing the chromaticity to increase above the nominal values.

REFERENCES

[1] R.P. Walker *et al.*, Diamond-II Technical Design Report, Aug 2022. https://www.diamond.ac.uk/Diamond-II.html

[2] N. Blaskovic Kraljevic, H. Ghasem, I.P.S. Martin and J. Kallestrup, "Multi-objective optimisation of the Diamond-II

storage ring optics", in *Proc. IPAC'25*, Taipei, Taiwan, June 2025, pp. 619–622. doi:10.18429/JACoW-IPAC2025-MOPS016.

[3] B. Nash *et al.*, "New functionality for beam dynamics in Accelerator Toolbox (AT)", in *Proc. IPAC'15*, Richmond, VA, USA, May 2015, pp. 113–116. doi:10.18429/JACoW-IPAC2015-MOPWA014

[4] N. Blaskovic Kraljevic, H. Ghasem and I. Martin, "Exploring the null space of the chromaticity response matrix at the Diamond Light Source", in *Proc. IPAC'25*, Taipei, Taiwan, June 2025, pp. 615–618. doi:10.18429/JACoW-IPAC2025-MOPS015.

[5] D. Rabusov, R. Fielder, S. Wang, and I. Martin, "Single-bunch instabilities and their mitigation in Diamond-II", in *Proc. IPAC'24*, Nashville, TN, USA, May 2024, pp. 786–789. doi:10.18429/JACoW-IPAC2024-MOPS33

[6] H. Bruck, *Accélérateurs circulaires de particules*, Presses Universitaires de France, Paris, 1966.

[7] N. Blaskovic Kraljevic, H.-C. Chao, H. Ghasem, I.P.S. Martin and S. Preston, "Numerical optimization of the Diamond-II storage ring optics", in *Proc. IPAC'24*, Nashville, TN, USA, May 2024, pp. 1254–1257. doi:10.18429/JACoW-IPAC2024-TUPG20

[8] A. Piwinski, "The Touschek effect in strong focusing storage rings", DESY, Hamburg, Germany, DESY Report No. DESY 98-179, 1998. doi:10.48550/arXiv.physics/9903034

[9] H. Ghasem, N. Blaskovic Kraljevic, B. Singh and I.P.S. Martin, "Lattice design for the Diamond-II light source storage ring", *Phys. Rev. Accel. Beams*, vol. 27, p. 110704, Nov. 2024. doi:10.1103/PhysRevAccelBeams.27.110704